Optically Induced Self-Excited Oscillations in an On-Fiber Optomechanical Cavity

Ilya Baskin, D. Yuvaraj, Gil Bachar, Keren Shlomi, Oleg Shtempluck, and Eyal Buks

Abstract— **Optically induced self-excited oscillations of suspended mirror of a fully on-fiber optomechanical cavity are experimentally demonstrated. The cavity is fabricated by patterning a suspended metallic mirror on the tip of an optical fiber and by introducing a static reflector in the fiber. We discuss the use of on-fiber optomechanical cavities for sensing applications. A theoretical analysis evaluates the sensitivity of the proposed sensor operating in the region of the self-excited oscillations. The results are compared with the experimental data and with the sensitivity that is achievable when the oscillations are driven by an external oscillatory force. [2013-0240]**

Index Terms— **Optomechanical cavity, optical fiber sensors.**

I. Introduction

OPTOMECHANICAL cavities, which are formed by coupling an optical cavity with a mechanical resonator, are currently a subject of intense basic and applied research [1, 2]. The optomechanical cavities can be employed in various sensing [3-6] and photonics applications [7-12] and may also allow an experimental study of basic physical effects (e.g. the crossover from classical to quantum mechanics [13, 14]).

When the finesse of the optical resonator that is employed for constructing the optomechanical cavity is sufficiently high, the coupling to the mechanical resonator that serves as a vibrating mirror is typically dominated by the effect of radiation pressure [1, 15-19]. On the other hand, bolometric effects can contribute to the optomechanical coupling when optical absorption by the vibrating mirror is significant [20-23]. In general, bolometric effects play an important role in relatively large mirrors, in which the thermal relaxation rate is comparable to the mechanical resonance frequency [24-27]. Phenomena such as mode cooling and self-excited oscillations [22, 25, 28-33] have been shown in systems in which bolometric effects are dominant [20-22, 24, 34, 35]

Recently, it was demonstrated that optomechanical cavities can be fabricated on the tip of an optical fiber [36, 42]. These miniature devices appear to be very promising for sensing applications. However, their operation requires external driving of the on-fiber mechanical resonator. Traditional driving using either electrical or magnetic actuation, however, is hard to implement with a mechanical resonator on the tip of an optical fiber; a limitation that can be overcome by optical actuation schemes [43].

In this paper we study a novel configuration of an on-fiber optomechanical cavity and demonstrate that self-excited oscillations can be optically induced by injecting a monochromatic laser light into the fiber. The optomechanical cavity is formed between the vibrating mirror that is fabricated on the tip of a single mode optical fiber and an additional static reflector which is introduced in the fiber. Optically-induced self-excited oscillations are attributed to the bolometric optomechanical coupling between the optical mode and the mechanical resonator and can be employed for resonator driving [34, 35].

The ability to induce self-excited oscillations can be exploited for operating an on-fiber optomechanical cavity as a sensor. Such a device can sense physical parameters that affect the resonance frequency of the suspended mirror (e.g. absorbed mass, acceleration, heating by external radiation, etc.). A sensor based on self-excited-oscillations effect is simple to fabricate and to operate, compact and robust. Moreover, the unneeded actuator coupling and circuitry might be beneficial fors future sensor applications. We present below the on-fiber optomechanical cavity showing self-excited oscillations, give a theoretical estimate of its sensitivity and compare it with the measured performance.

II. Experiment

The optomechanical cavity shown in Fig. 1 was fabricated on the flat polished tip of a single mode fused silica optical fiber having outer diameter of $126\,\mu$m (Corning SMF-28 operating at wavelength $\lambda_0 \approx 1550\,$nm) held in a zirconia ferrule. A 10 nm-thick chromium layer and a 200 nm gold layer were deposited successively by thermal evaporation. The bi-layer was directly patterned by a focused ion beam to the desired mirror shape ($20\,\mu$m-wide doubly clamped beam). Finally, the mirror was released by etching approximately $12\,\mu$m of the underlying silica in 7% HF acid (90 min etch time at room temperature). The beam remained supported by

Manuscript received July 31, 2013; revised October 19, 2013; accepted October 27, 2013. Date of publication November 20, 2013; date of current version May 29, 2014. This work was supported in part by the German Israel Foundation under Grant 1-2038.1114.07, in part by the Israel Science Foundation, in part by the Bi-National Science Foundation, in part by the Deborah Foundation, in part by the Shulman Foundation, in part by the Mitchel Foundation, in part by the Israel Ministry of Science, in part by the Russell Berrie Nanotechnology Institute, in part by the European STREP QNEMS Project, in part by the MAGNET Metro 450 consortium, and in part by MAFAT. The work of I. Baskin was supported by a Zeff Fellowship. Subject Editor S. Merlo.

The authors are with the Department of Electrical Engineering, Technion–Israel Institute of Technology, Haifa 32000, Israel (e-mail: ilbaskin@tx.technion.ac.il; yuvaraj@gmail.com; bachargil@gmail.com; shlomps@gmail.com; shot@techunix.technion.ac.il; eyal@ee.technion.ac.il).

Color versions of one or more of the figures in this paper are available online at http://ieeexplore.ieee.org.

Digital Object Identifier 10.1109/JMEMS.2013.2290061

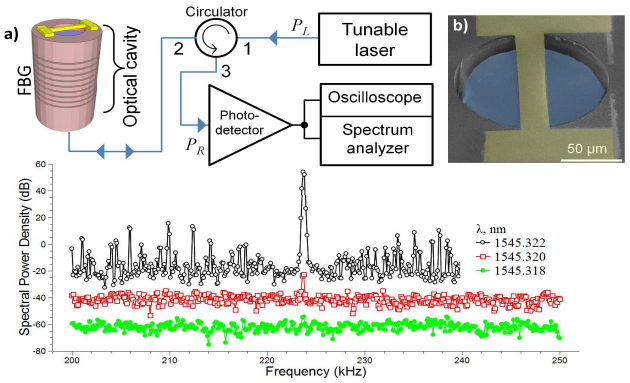

Fig. 1. (a) A schematic drawing of the sample and the experimental set-up. On-fiber optomechanical cavity is excited by a tunable laser. The reflected light intensity is measured and analyzed. (b) Electron micrograph of a suspended micromechanical mirror (false color code: blue-silica fiber, yellow - gold mirror, gray - zirconia ferrule), the view is tilted by 52°. (c) Spectral decomposition of the reflected light power (P_R) vs. excitation wavelengths. High amplitude oscillations of the P_R (visible as an intense peak in the spectrum) correspond to self-excited oscillations. Curves corresponding to $\lambda = 1545.322$ nm and $\lambda = 1545.320$ nm are shifted vertically for clarity.

the zirconia ferrule, which is resistant to HF. The precise alignment between the micro-mechanical mirror and fiber core that was achieved in the fabrication process allowed robust and simple operation without a need of any post-fabrication positioning.

The static mirror of the optomechanical cavity was provided by a fiber Bragg grating (FBG) mirror (made using a standard phase mask technique [44], grating period of 0.527 μm and length $\approx$ 8 mm) with the reflectivity band of 0.4 nm FWHM centered at λ_0. The length of the optical cavity was $l \approx 10$ mm providing a free spectral range $\Delta\lambda = \lambda_0^2/2n_{\text{eff}}l \approx 80$ pm (where $n_{\text{eff}} = 1.468$ is the effective refraction index for SMF-28). The cavity length was chosen so that at least five cavity resonance wavelengths would be located within the range of the FBG reflectivity band. Despite of the high FBG reflectivity ($\approx$ 90%) the resulting cavity finesse was low (about 2) due to the high cavity losses (see Ref. [34] for detailed discussion of the cavity reflectivity spectrum). The most plausible source of losses is the light scattering on the rough etched fiber tip surface (protuberances of micron size were observed below the suspended beam), giving rise to radiation loss.

Monochromatic light was injected into the fiber bearing the cavity on its tip from a laser source with an adjustable output wavelength (λ, tunable in the range of 1525–1575 nm) and power level (P_L, up to 20 mW). The laser was connected through an optical circulator, that allowed the measurement of the reflected light intensity (P_R) by a fast responding photodetector. The detected signal was analyzed by an oscilloscope and a spectrum analyzer (see the schematics at Fig. 1(a). The experiments were performed in vacuum (at residual pressure below 10 mPa) with sample thermally anchored to a cold finger with temperature adjustable between 4 to 300 K. The resonance frequency of the suspended mirror, ω_0 was estimated by the frequency of thermal oscillations measured at low input laser power. (At power levels well below the self-excited oscillations threshold the mechanical and optical systems are effectively decoupled [34].)

The spectral decomposition of the reflected signal power $P_R(f)$, measured for $\lambda = 1545.318$, 1545.320 and 1545.322 nm (curves marked by empty circles, squares and filed circles, respectively) is shown in Fig. 1(c). The appearance of a striking peak in $P_R(f)$ spectrum (measured at $\lambda = 1545.322$ nm) indicates the onset of self-excited oscillations. The mechanical origin of these oscillations was verified by observation of the spectral peak broadening induced by a deliberate reduction of the mechanical quality factor (by increasing the drag friction by venting the vacuum chamber with atmospheric air). When the air pressure was increased to 1 atm, the peak of Fig. 1(c) became over-broaden and was obscured by the measurement noise.

The $P_R(f, \lambda)$ spectrum (shown as a color-map in Fig. 2(a) was measured for the wavelength range covering the sample reflectivity band. The sharp spectral peaks that appear just below the mechanical resonance frequency ω_0 (marked by a dotted line in Fig. 2(a) correspond to the self-excited oscillations of the vibrating mirror. These oscillations are "turned on" when the laser wavelength is adjusted to the specific regions of the cavity's reflectivity spectrum ($R(\lambda)$, blue curve in Fig. 2(b) and P_L exceeds a (wavelength dependent) threshold value.

Some interesting observations can be made by inspection of Fig. 2. (1) The self-excited oscillations appear at wavebands having positive slope of reflectivity vs. wavelength. In other words, self-excited oscillations are induced by a light that is "red-detuned" from the cavity resonance. Note that, in contrast, in dispersively coupled optomechanical systems self-excited oscillations can only be induced by "blue-detuned" light [1]. (2) The self-excited oscillation frequency significantly varies as a function of λ. (3) The step-like onset of the oscillations amplitude as a function of λ (sweeping through the region of self-excited oscillations, black solid line in Fig. 2(b) indicates a threshold behavior of optomechanical system. We will refer to these observations further, in the framework of the model developed in Section IV.

III. Resonant Detection

To estimate the sensitivity of a sensor that is based on optomechanical cavity, the phase noise of the self-excited oscillations is theoretically evaluated below. In general, the resonant detection with a mechanical resonator is a widely employed technique in a variety of applications [45-48]. A detector belonging to this class typically consists of a mechanical resonator, which is characterized by an angular resonance frequency Ω and characteristic damping rate Γ. Detection is achieved by coupling the measured physical parameter of interest, denoted as p, to the resonator in such a way that Ω becomes effectively p-dependent, i.e. $\Omega = \Omega(p)$. The sensitivity of the detection scheme that is employed for monitoring the parameter p can be characterized by the minimum detectable change in p, denoted as δp. For small changes, δp is related to the normalized minimum detectable change in the frequency $\sigma_y = \delta\Omega/\Omega$ by the relation $\delta p = |\partial\Omega/\partial p|^{-1}\,\Omega\sigma_y$. The dimensionless parameter σ_y, in turn, typically depends on

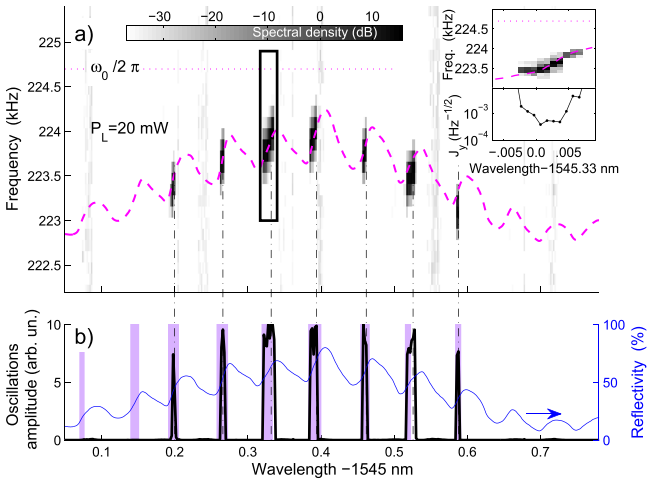

Fig. 2. (a) Spectral power density of the reflected optical power as function of frequency and excitation wavelength. The self-excited oscillations are seen as sharp peaks in the reflected power spectrum (dark-gray regions of the colormap). The effective resonance frequency fit by Eq. (10) (dashed curve) and the uncoupled mechanical oscillator resonance frequency (dotted line) are shown. Inset: zoom-in to a self-excited oscillations peak (marked by a rectangle) and the sensitivity factor estimation J_y. (b) The reflected power oscillations amplitude (black solid curve) and the wavelength bands where the self-excited oscillations are expected ($\Gamma_0 < 0$ in Eq. (20), indicated by the pink bars). Fitting curves of panels a) and b) are based on the sample reflectivity spectrum (blue curve on panel b) and the following experimental parameters: $\omega_0/2\pi = 2.2465 \times 10^5$ $\gamma_0/2\pi = 50$ Hz, $\kappa = 12.0 \times 10^3$ Hz, $\beta = 2.2\times10^3$ s^{-1} K^{-1}, $\theta = -14\times10^3$ N kg^{-1} K^{-1} and $\eta = 3.5\times10^6$ K J^{-1}.

the noise in the system and on the averaging time τ that is employed for the measurement. For a detection scheme based on forced oscillations the normalized minimum detectable change in the frequency (σ_y) is found to be given by [49]

$$\sigma_y = \left(\frac{2\Gamma k_B T_{eff}}{U_0 \Omega^2 \tau}\right)^{1/2}, \tag{1}$$

where k_B is the Boltzmann's constant, T_{eff} is the noise effective temperature and U_0 is the energy stored in the externally driven resonator in steady state. It is convenient to define the sensitivity factor $J_y = \sigma_y \tau^{1/2}$ that does not depend on the integration time [see Eq.(1)] and can be used to compare detectors measured in different experimental conditions. Note that Eq. (1) is derived for a linear resonator in the classical limit ($k_B T_{eff} \gg \hbar\Omega$). The generalization of Eq. (1) for the case of nonlinear response is discussed in Ref. [50].

IV. Model and Discussion

In the limit of small displacement, the dynamics of the system can be approximately described using a single evolution equation [35]. The theoretical model that is used to derive the evolution equation is briefly described below. Note that some optomechanical effects that were taken into account in the theoretical modeling [35] were found experimentally to have a negligible effect on the dynamics [34] (e.g. the effect of radiation pressure). In what follows such effects are disregarded.

The micromechanical mirror in the optical cavity is treated as a mechanical resonator with a single degree of freedom x having mass m and damping rate γ_0 (when it is decoupled from the optical cavity). It is assumed that the angular resonance frequency (ω_m) of the mechanical resonator depends on the temperature T of the suspended mirror. For small deviation of T from the base temperature T_0 (i.e. the temperature of the supporting substrate) ω_m is taken to be given by

$$\omega_m = \omega_0 - \beta\,(T - T_0)\,, \tag{2}$$

where β is a constant. Furthermore, to model the effect of thermal deformation it is assumed that a temperature dependent force given by

$$F_{th} = \theta\,(T - T_0)\,, \tag{3}$$

where θ is a constant, acts on the mechanical resonator [22]. The mechanical oscillator's equation of motion is given by

$$\ddot{x} + 2\gamma_0\dot{x} + \omega_m^2(T)x = F_{th}(T), \tag{4}$$

where an overdot denotes differentiation with respect to time.

The time evolution of the effective temperature T is governed by the thermal balance equation

$$\dot{T} = \kappa\,(T_0 - T) + \eta P_L I\,(x)\,, \tag{5}$$

where η is the heating coefficient due to optical absorption, κ is the thermal rate, P_L is the injected laser power and $P_L I\,(x)$ is the intra-cavity optical power incident on the suspended mirror, which depends on the mechanical displacement x (i.e. on the length of the optical cavity) due to the effect of optical interference.

For small x the expansion

$$I\,(x) \simeq I_0 + I_0' x + (1/2)\,I_0'' x^2 \tag{6}$$

is employed, where a prime denotes differentiation with respect to the displacement x. This model neglects the mechanical nonlinearities of the resonator, i.e. it is assumed that nonlinear behavior exclusively originates from bolometric optomechanical coupling.

The displacement $x\,(t)$ can be expressed in terms of the complex amplitude A as

$$x\,(t) = x_0 + 2\,\mathrm{Re}\,A, \tag{7}$$

where x_0, which is given by $x_0 = \eta\theta P_L I_0/\kappa\omega_0^2$, is the optically-induced static displacement. For small displacement, the evolution equation for the complex amplitude A is found to be given by the following Langevin equation [35]

$$\dot{A} + (\Gamma_{eff} + i\Omega_{eff})\,A = \xi\,(t)\,, \tag{8}$$

where both the effective resonance frequency Ω_{eff} and the effective damping rate Γ_{eff} are real even functions of $|A|$. To second order in $|A|$ they are given by

$$\Gamma_{eff} = \gamma_0 + \frac{\eta\theta P_L}{2\omega_0^2} I_0' + \frac{\eta\beta P_L}{4\omega_0} I_0''\,|A|^2\,, \tag{9}$$

$$\Omega_{eff} = \omega_0 - \frac{\eta\beta P_L}{\kappa} I_0 - \frac{\eta\beta P_L}{\kappa} I_0''\,|A|^2\,. \tag{10}$$

The above expressions for Γ_{eff} and Ω_{eff} are obtained by making the following assumptions $\beta x_0 \ll \theta/2\omega_0$, $\theta\kappa^2 \ll \beta\omega_0^3\lambda$ and $\kappa \ll \omega_0$, which typically hold experimentally [34]. The fluctuating term [51]

$$\xi\,(t) = \xi_x\,(t) + i\xi_y\,(t)\,, \tag{11}$$

where both ξ_x and ξ_y are real, represents white noise and the following is assumed to hold

$$\langle \xi_x(t_1)\,\xi_x(t_2)\rangle = 2\Theta\delta(t_1-t_2), \tag{12}$$

$$\langle \xi_y(t_1)\,\xi_y(t_2)\rangle = 2\Theta\delta(t_1-t_2), \tag{13}$$

$$\langle \xi_x(t_1)\,\xi_y(t_2)\rangle = 0, \tag{14}$$

where $\Theta = \gamma_0 k_B T_{\text{eff}}/4m\omega_0^2$ and where T_{eff} is the effective noise temperature.

The self-excited oscillations frequency variation as a function of λ was fitted by Eq. (10) (dashed curve in Fig. 2(a) using β as a fitting parameter. To preform the fit we estimated the power absorbed by the beam ($P_L I_0$) from the reflection spectrum and the nonlinear term of the Eq. (10) was neglected. The good agreement with data that is obtained from fitting procedure shows that self-excited oscillations frequency variation stems mainly from beam heating.

In cylindrical coordinates A is expressed as

$$A = A_r e^{iA_\theta}, \tag{15}$$

where $A_r = |A|$ and A_θ is real [52]. The equations of motion for A_r and for A_θ are given by [see Eq. (8)]

$$\dot{A}_r + A_r\Gamma_{\text{eff}} = \xi_r(t), \tag{16}$$

and

$$\dot{A}_\theta + \Omega_{\text{eff}}(A_r) = \xi_\theta(t)/A_r, \tag{17}$$

where the fluctuating terms satisfy the following relations

$$\langle \xi_\theta(t_1)\,\xi_\theta(t_2)\rangle = 2\Theta\delta(t_1-t_2), \tag{18}$$

$$\langle \xi_r(t_1)\,\xi_\theta(t_2)\rangle = 0. \tag{19}$$

By introducing the notation

$$\Gamma_0 = \gamma_0 + \eta\theta P_L I_0'/2\omega_0^2 \tag{20}$$

and

$$\Gamma_2 = \eta\beta P_L I_0''/4\omega_0 \tag{21}$$

one can express the effective damping rate Γ_{eff} as [see Eq. (9)]

$$\Gamma_{\text{eff}} = \Gamma_0 + \Gamma_2 A_r^2. \tag{22}$$

Consider the case where $\theta I_0' < 0$ and where $\beta I_0'' > 0$. For such a case a supercritical Hopf bifurcation occurs when Γ_0 vanishes, i.e. for a critical value of the laser power given by $P_{\text{LC}} = -2\omega_0^2\gamma_0/\eta\theta I_0'$. The self-excited oscillations emerge above the threshold, i.e. when Γ_0 becomes negative.

In many optomechanical systems the light stored in optical cavity acts to reduce the optical resonance frequency by lengthening the cavity. This is always the case for the radiation pressure coupled optomechanical cavities. For the bolometric coupling, on the other hand, this is the case only when $\theta > 0$. However, θ may take negative values due to beam buckling effects and consequently self-excited oscillations are possible only for the wavebands corresponding to $dI/dx > 0$ (i.e. "red detuning" as in Fig. 2(b) [53]. We note that the observation of the self-excited oscillations for "red-detuned" laser input eliminates the possibility of the dispersive coupling mechanism in the optomechanical cavity. A detailed study of optomechanical cavity comprised of buckled mirror has been published [53].

A reasonably good fit of the wavebands supporting self-excited oscillations was achieved by solving $\Gamma_0 < 0$ for λ, while θ is taken as a fit parameter. The solution is mapped in Fig. 2(b) as pink bars (with oscillation amplitude curve). For two wavebands around $\lambda = 1545.072$ and 1545.144 nm the self-excited oscillations do not appear in experiment despite the fact that Γ_0 was estimated to be negative. We consider that the saturation of the photo-detector response led to "flattening" of central lobes of the reflectivity spectrum and to overestimation of the effective damping rate variation at side-lobes.

The steady state value of A_r (when noise is disregarded) is given by $r_0 = \sqrt{-\Gamma_0/\Gamma_2}$. In terms of the laser power r_0 can be expressed as

$$r_0 = \lambda\sqrt{-\frac{2\theta}{\beta\omega_0\lambda}\frac{I_0'}{\lambda I_0''}\frac{\Delta P_L}{P_L}}, \tag{23}$$

where $\Delta P_L = P_L - P_{LC}$.

Using the notation

$$A_r = r_0 + \rho, \tag{24}$$

one finds to lowest nonvanishing order in ρ that $A_r\Gamma_{\text{eff}} = -2\Gamma_0\rho + O(\rho^2)$. Moreover $\Omega_{\text{eff}} = \Omega_H + \zeta\rho + O(\rho^2)$, where $\Omega_H = \Omega_{\text{eff}}(r_0)$ and where $\zeta = d\Omega_{\text{eff}}/dA_r$ at the point r_0. To lowest nonvanishing order in ρ the equations of motion for A_r and A_θ become

$$\dot{\rho} - 2\Gamma_0\rho = \xi_r(t) \tag{25}$$

and

$$\dot{\phi} + \zeta\rho = \frac{\xi_\theta(t)}{r_0}, \tag{26}$$

where $\phi = A_\theta + \Omega_H t$. In steady state (i.e. in the limit $t \to \infty$) the solution for ρ reads

$$\rho(t) = \int_0^t e^{2\Gamma_0(t-t_1)}\xi_r(t_1)\,dt_1. \tag{27}$$

The correlation function of $\rho(t)$ is $\langle \rho(t_1)\,\rho(t_2)\rangle = -\left(\Theta/2\Gamma_0\right) e^{2\Gamma_0|t_1-t_2|}$, and thus the autocorrelation function of $\dot{\phi}$ is given by

$$\langle \dot{\phi}(t_1)\,\dot{\phi}(t_2)\rangle = \Theta\left[\frac{\zeta^2 e^{2\Gamma_0|t_1-t_2|}}{2|\Gamma_0|} + 2\frac{\Gamma_2}{|\Gamma_0|}\delta(t_1-t_2)\right]. \tag{28}$$

The power spectrum $S_{\dot{\phi}}(\omega)$ of $\dot{\phi}$ can be directly evaluated from Eq. (28) using Wiener-Khinchine theorem [54], which relates auto correlation function with spectral density,

$$S_{\dot{\phi}}(\omega) = \frac{1}{\pi}\frac{\Theta\zeta^2}{4\Gamma_0^2+\omega^2} + \frac{\Theta\Gamma_2}{\pi|\Gamma_0|}. \tag{29}$$

The signal

$$y(t) \equiv \dot{\phi}/\Omega_H \tag{30}$$

represents the normalized the momentary angular frequency $\Omega_H + \dot{\phi}$. The average value of $y(t)$ is estimated by monitoring the signal $y(t)$ in a time interval τ:

$$\hat{y}(\tau) = \frac{1}{\tau}\int_{-\tau/2}^{\tau/2} dt\; y(t). \tag{31}$$

In the limit of steady state, i.e. when $\tau \gg 1/|\Gamma_0|$, the variance of the estimator $\hat{y}(\tau)$, which is proportional to the

minimal detectable frequency change, is given by $\sigma_y^2(\tau) = 2\pi S_y(0)/\tau$, thus

$$\sigma_y^2(\tau) = \frac{2\Theta}{\Omega_H^2 r_0^2 \tau}\left(1 + \frac{\zeta^2}{4|\Gamma_0|\Gamma_2}\right). \quad (32)$$

Note that due to the fact that in the present case $S_{\dot{\phi}}(\omega)$ remains finite in the limit $\omega \to 0$, the above defined variance $\sigma_y^2(\tau)$ is identical to the Allan variance [55]–[57]. With the help of Eq. (10) one finds that $\zeta^2/4|\Gamma_0|\Gamma_2 = (4\omega_0/\kappa)^2$. The assumption that $\kappa \ll \omega_0$ [34] leads to

$$\sigma_y(\tau) = \frac{4\omega_0}{\kappa}\left(\frac{2\gamma_0 k_B T_{eff}}{U_0 \omega_0^2 \tau}\right)^{1/2}, \quad (33)$$

where $U_0 = 4m\Omega_H^2 r_0^2$ is the energy stored in the self-excited resonator in steady state close to the threshold. The comparison with Eq. (1) indicates that $\sigma_y(\tau)$ for the case of optically induced self-excited oscillations is roughly $4\omega_0/\kappa$ times larger compared with the case of external drive for the same values of U_0 and T_{eff}. Generally bolometrically coupled optomechanical cavities support the self-excited oscillations only if the thermal relaxation rate is lower than the oscillator resonance frequency (i.e. sufficient retardation between the mechanical mirror movement and the thermal force variation is provided [22], [34], [35]). For the optomechanical devices under study the ratio ω_0/κ is about 100.

The factor J_y as a function of P_L was experimentally measured using an on-fiber optomechanical cavity device, in which the mechanical mirror covers almost the entire fiber cross section (schematically shown in the inset of Fig. 3). In this device self-excited oscillations as a function of input power were observed above a threshold value of $P_L = 8.7$ mW [see Fig. 3]. To experimentally determine the factor J_y, the reflected optical power was recorded over a time period of 2 ms using an oscilloscope. The factor σ_y, which was found by the zero-crossing technique [56], allowed evaluation of J_y.

The frequency of self-excited oscillations $\Omega_H/2\pi$, the sensitivity factor J_y and oscillations amplitude are plotted vs. laser power P_L in panels (a), (b) and (c) of Fig. 3, respectively. The experimental data is shown by star marks, while a theoretical fit that is based on Eqs. (10), (33) and (23) is shown by the red solid lines. Since the presented model is only valid in the small amplitude limit i.e. for P_L just above the threshold, the theoretical curve was limited to the maximal range for which a reasonable fit can be achieved. Noticeably, J_y continues to decrease with increasing P_L even beyond the range that is covered by our approximated model. The experimental parameters that have been employed in the curve fitting are listed in the figure caption.

The sensitivity factor (in the self-excited oscillations regime) was evaluated for a number of on-fiber optomechanical cavities of various geometries (e.g. J_y data shown in the inset of Fig. 2) and for cavities comprising an optical fiber actively aligned against a suspended micro-mirror (as in preceding work by Zaitsev et al. [34]). The sensitivity of these devices was of the same order of magnitude as in the data seen in Fig. 3(b).

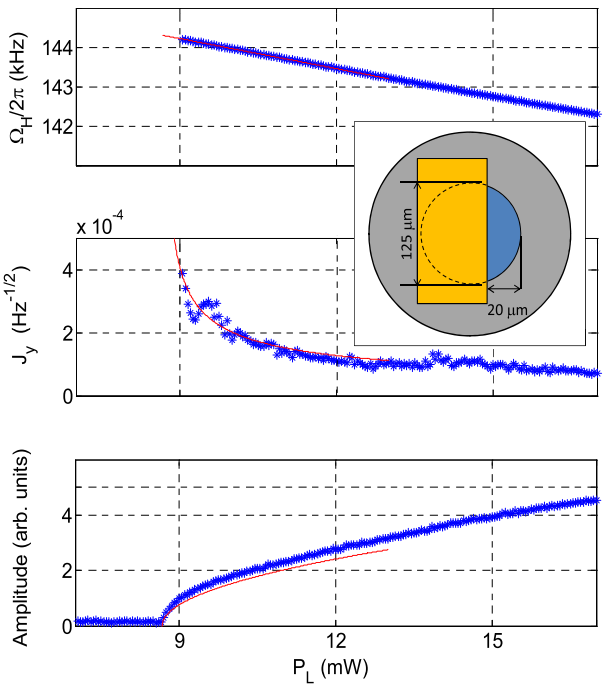

Fig. 3. The frequency of self-excited oscillations $\Omega_H/2\pi$ [panel (a)], the sensitivity factor J_y [panel (b)] and oscillations amplitude [panel (c)] vs. laser power P_L. The star marks represent experimental data, the solid lines represent a theoretical fit that is based on the following experimental parameters: $\kappa = 22 \times 10^3$ Hz, $m = 30 \times 10^{-12}$ kg, $\lambda = 1.55\,\mu$m, $T_{eff} = 300$ K, $\Omega/\Gamma = 10^3$, $|I_0'|/\lambda I_0'' = 0.8$, $\beta = 10^4$ s^{-1} K^{-1}, $\theta = 1.6 \times 10^3$ N kg^{-1} K^{-1} and $\eta = 3.5 \times 10^6$ K J^{-1}. Inset: sample schematics (top-view, not to scale). Yellow - suspended membrane, blue - the fiber top, gray - ferrule.

V. Conclusion

Optically induced self-excited oscillations of the suspended mirror fabricated on the optical fiber tip were experimentally demonstrated. Based on previously developed model of bolometrically coupled optomechanical cavity we estimated the sensitivity of a detector exploiting the self-excited oscillations effect. The estimations predict an inherent loss of the sensitivity (compared to traditional externally actuated resonator). However, the fabrication and operation simplicity of self-excited optomechanical detectors in many cases compensates the possible degradation in the sensitivity and can be very attractive for future sensor applications.

References

[1] T. J. Kippenberg and K. J. Vahala, "Cavity optomechanics: Back-action at the mesoscale," *Science*, vol. 321, pp. 1172–1176, Aug. 2008.
[2] F. Marquardt and S. M. Girvin, "Trend: Optomechanics," *Physics*, vol. 2, p. 40, May 2009.
[3] D. Rugar, H. J. Mamin, and P. Guethner, "Improved fiber-optic interferometer for atomic force microscopy," *Appl. Phys. Lett.*, vol. 55, no. 25, pp. 2588–2590, 1989.
[4] O. Arcizet, P.-F. Cohadon, T. Briant, M. Pinard, A. Heidmann, J.-M. Mackowski, *et al.*, "High-sensitivity optical monitoring of a micromechanical resonator with a quantum-limited optomechanical sensor," *Phys. Rev. Lett.*, vol. 97, no. 13, pp. 133601-1–133601-4, Sep. 2006.
[5] S. Forstner, S. Prams, J. Knittel, E. D. van Ooijen, J. D. Swaim, G. I. Harris, *et al.*, "Cavity optomechanical magnetometer," *Phys. Rev. Lett.*, vol. 108, pp. 120801-1–120801-5, Mar. 2012.
[6] S. Stapfner, L. Ost, D. Hunger, J. Reichel, I. Favero, and E. M. Weig, "Cavity-enhanced optical detection of carbon nanotube Brownian motion," *Appl. Phys. Lett.*, vol. 102, no. 15, pp. 151910-1–151910-5, 2013.

[7] N. Stokes, F. Fatah, and S. Venkatesh, "Self-excited vibrations of optical microresonators," *Electron. Lett.*, vol. 24, no. 13, pp. 777–778, 1988.

[8] M. Hossein-Zadeh and K. J. Vahala, "An optomechanical oscillator on a silicon chip," *IEEE J. Sel. Topics Quantum Electron.*, vol. 16, no. 1, pp. 276–287, Jan. 2010.

[9] M. C. Wu, O. Solgaard, and J. E. Ford, "Optical MEMS for lightwave communication," *J. Lightw. Technol.*, vol. 24, no. 12, pp. 4433–4454, Dec. 2006.

[10] M. Eichenfield, C. P. Michael, R. Perahia, and O. Painter, "Actuation of micro-optomechanical systems via cavity-enhanced optical dipole forces," *Nature Photon.*, vol. 1, pp. 416–422, Jul. 2007.

[11] G. Bahl, J. Zehnpfennig, M. Tomes, and T. Carmon, "Stimulated optomechanical excitation of surface acoustic waves in a microdevice," *Nature Commun.*, vol. 2, p. 403, Jul. 2011.

[12] N. Flowers-Jacobs, S. Hoch, J. Sankey, A. Kashkanova, A. Jayich, C. Deutsch, *et al.*, "Fiber-cavity-based optomechanical device," *Appl. Phys. Lett.*, vol. 101, no. 22, pp. 221109-1–221109-4, 2012.

[13] J. Thompson, B. Zwickl, A. Jayich, F. Marquardt, S. Girvin, and J. Harris, "Strong dispersive coupling of a high-finesse cavity to a micromechanical membrane," *Nature*, vol. 452, no. 7183, pp. 72–75, 2008.

[14] P. Meystre, "A short walk through quantum optomechanics," *Ann. Phys.*, vol. 525, no. 3, pp. 215–233, 2013.

[15] T. J. Kippenberg, H. Rokhsari, T. Carmon, A. Scherer, and K. J. Vahala, "Analysis of radiation-pressure induced mechanical oscillation of an optical microcavity," *Phys. Rev. Lett.*, vol. 95, pp. 033901-1–033901-4, Jul. 2005.

[16] H. Rokhsari, T. Kippenberg, T. Carmon, and K. Vahala, "Radiation-pressure-driven micro-mechanical oscillator," *Opt. Express*, vol. 13, pp. 5293–5301, Jul. 2005.

[17] O. Arcizet, P. F. Cohadon, T. Briant, M. Pinard, and A. Heidmann, "Radiation-pressure cooling and optomechanical instability of a micromirror," *Nature*, vol. 444, pp. 71–74, Nov. 2006.

[18] S. Gigan, H. R. Böhm, M. Paternostro, F. Blaser, G. Langer, J. B. Hertzberg, *et al.*, "Self-cooling of a micromirror by radiation pressure," *Nature*, vol. 444, pp. 67–70, Nov. 2006.

[19] D. Kleckner and D. Bouwmeester, "Sub-kelvin optical cooling of a micromechanical resonator," *Nature*, vol. 444, pp. 75–78, Nov. 2006.

[20] C. H. Metzger and K. Karrai, "Cavity cooling of a microlever," *Nature*, vol. 432, pp. 1002–1005, Dec. 2004.

[21] G. Jourdan, F. Comin, and J. Chevrier, "Mechanical mode dependence of bolometric backaction in an atomic force microscopy microlever," *Phys. Rev. Lett.*, vol. 101, pp. 133904-1–133904-4, Sep. 2008.

[22] C. Metzger, M. Ludwig, C. Neuenhahn, A. Ortlieb, I. Favero, K. Karrai, *et al.*, "Self-induced oscillations in an optomechanical system driven by bolometric backaction," *Phys. Rev. Lett.*, vol. 101, pp. 133903-1–133903-4, Sep. 2008.

[23] F. Marino and F. Marin, "Chaotically spiking attractors in suspended-mirror optical cavities," *Phys. Rev. E*, vol. 83, pp. 015202-1–015202-4, Jan. 2011.

[24] K. Aubin, M. Zalalutdinov, T. Alan, R. Reichenbach, R. Rand, A. Zehnder, *et al.*, "Limit cycle oscillations in CW laser-driven NEMS," *J. Microelectromech. Syst.*, vol. 13, pp. 1018–1026, Dec. 2004.

[25] F. Marquardt, J. G. E. Harris, and S. M. Girvin, "Dynamical multistability induced by radiation pressure in high-finesse micromechanical optical cavities," *Phys. Rev. Lett.*, vol. 96, no. 10, pp. 103901-1–103901-4, 2006.

[26] M. Paternostro, S. Gigan, M. S. Kim, F. Blaser, H. R. Böhm, and M. Aspelmeyer, "Reconstructing the dynamics of a movable mirror in a detuned optical cavity," *New J. Phys.*, vol. 8, pp. 107–108, Jun. 2006.

[27] S. De Liberato, N. Lambert, and F. Nori, "Quantum noise in photothermal cooling," *Phys. Rev. A*, vol. 83, pp. 033809-1–033809-7, Mar. 2011.

[28] K. Hane and K. Suzuki, "Self-excited vibration of a self-supporting thin film caused by laser irradiation," *Sens. Actuators A, Phys.*, vol. 51, nos. 2–3, pp. 179–182, 1996.

[29] K. Kim and S. Lee, "Self-oscillation mode induced in an atomic force microscope cantilever," *J. Appl. Phys.*, vol. 91, no. 7, pp. 4715–4719, 2002.

[30] K. Aubin, M. Zalalutdinov, T. Alan, R. Reichenbach, R. Rand, A. Zehnder, *et al.*, "Limit cycle oscillations in CW laser-driven NEMS," *J. Microelectromech. Syst.*, vol. 13, no. 6, pp. 1018–1026, 2004.

[31] T. Carmon, H. Rokhsari, L. Yang, T. J. Kippenberg, and K. J. Vahala, "Temporal behavior of radiation-pressure-induced vibrations of an optical microcavity phonon mode," *Phys. Rev. Lett.*, vol. 94, no. 22, pp. 223902-1–223902-4, 2005.

[32] T. Corbitt, D. Ottaway, E. Innerhofer, J. Pelc, and N. Mavalvala, "Measurement of radiation-pressure-induced optomechanical dynamics in a suspended Fabry–Perot cavity," *Phys. Rev. A*, vol. 74, no. 2, pp. 021802R-1–021802R-4, 2006.

[33] T. Carmon and K. J. Vahala, "Modal spectroscopy of optoexcited vibrations of a micron-scale on-chip resonator at greater than 1 GHz frequency," *Phys. Rev. Lett.*, vol. 98, no. 12, pp. 123901-1–123901-4, 2007.

[34] S. Zaitsev, A. K. Pandey, O. Shtempluck, and E. Buks, "Forced and self-excited oscillations of an optomechanical cavity," *Phys. Rev. E*, vol. 84, no. 4, pp. 046605-1–046605-10, 2011.

[35] S. Zaitsev, O. Gottlieb, and E. Buks, "Nonlinear dynamics of a micro-electromechanical mirror in an optical resonance cavity," *Nonlinear Dyn.*, vol. 69, no. 4, pp. 1589–1610, 2012.

[36] D. Iannuzzi, S. Deladi, V. J. Gadgil, R. G. P. Sanders, H. Schreuders, and M. C. Elwenspoek, "Monolithic fiber-top sensor for critical environments and standard applications," *Appl. Phys. Lett.*, vol. 88, no. 5, pp. 053501-1–053501-3, 2006.

[37] C. Ma and A. Wang, "Optical fiber tip acoustic resonator for hydrogen sensing," *Opt. Lett.*, vol. 35, pp. 2043–2045, Jun. 2010.

[38] D. Chavan, G. Gruca, S. de Man, M. Slaman, J. H. Rector, K. Heeck, *et al.*, "Ferrule-top atomic force microscope," *Rev. Sci. Instrum.*, vol. 81, no. 12, pp. 123702-1–123702-5, 2010.

[39] K. B. Gavan, J. H. Rector, K. Heeck, D. Chavan, G. Gruca, T. H. Oosterkamp, *et al.*, "Top-down approach to fiber-top cantilevers," *Opt. Lett.*, vol. 36, pp. 2898–2900, Aug. 2011.

[40] I. W. Jung, B. Park, J. Provine, R. Howe, and O. Solgaard, "Highly sensitive monolithic silicon photonic crystal fiber tip sensor for simultaneous measurement of refractive index and temperature," *J. Lightw. Technol.*, vol. 29, no. 9, pp. 1367–1374, May 1, 2011.

[41] A. Butsch, M. S. Kang, T. G. Euser, J. R. Koehler, S. Rammler, R. Keding, *et al.*, "Optomechanical nonlinearity in dual-nanoweb structure suspended inside capillary fiber," *Phys. Rev. Lett.*, vol. 109, pp. 183904-1–183904-5, Nov. 2012.

[42] F. Albri, J. Li, R. R. J. Maier, W. N. MacPherson, and D. P. Hand, "Laser machining of sensing components on the end of optical fibres," *J. Micromech. Microeng.*, vol. 23, no. 4, pp. 45021–45028, 2013.

[43] G. Gruca, D. Chavan, J. Rector, K. Heeck, and D. Iannuzzi, "Demonstration of an optically actuated ferrule-top device for pressure and humidity sensing," *Sens. Actuators A, Phys.*, vol. 190, pp. 77–83, Feb. 2013.

[44] D. Z. Anderson, V. Mizrahi, T. Erdogan, and A. White, "Production of in-fibre gratings using a diffractive optical element," *Electron. Lett.*, vol. 29, no. 6, pp. 566–568, 1993.

[45] T. Larsen, S. Schmid, L. Grönberg, A. O. Niskanen, J. Hassel, S. Dohn, *et al.*, "Ultrasensitive string-based temperature sensors," *Appl. Phys. Lett.*, vol. 98, no. 12, pp. 121901-1–121901-3, 2011.

[46] B. Ilic, H. G. Craighead, S. Krylov, W. Senaratne, and C. Ober, "Attogram detection using nanoelectromechanical oscillators," *J. Appl. Phys.*, vol. 95, pp. 3694–3703, Apr. 2004.

[47] A. N. Cleland, "Thermomechanical noise limits on parametric sensing with nanomechanical resonators," *New J. Phys.*, vol. 7, no. 1, p. 235, 2005.

[48] A. K. Pandey, O. Gottlieb, O. Shtempluck, and E. Buks, "Performance of an AuPd micromechanical resonator as a temperature sensor," *Appl. Phys. Lett.*, vol. 96, no. 20, pp. 203105-1–203105-3, 2010.

[49] A. N. Cleland and M. L. Roukes, "Noise processes in nanomechanical resonators," *J. Appl. Phys.*, vol. 92, pp. 2758–2769, Sep. 2002.

[50] E. Buks, S. Zaitsev, E. Segev, B. Abdo, and M. P. Blencowe, "Displacement detection with a vibrating RF SQUID: Beating the standard linear limit," *Phys. Rev. E*, vol. 76, no. 2, pp. 026217-1–026217-10, 2007.

[51] H. Risken, *The Fokker-Planck Equation: Methods of Solution and Applications*. New York, NY, USA: Springer-Verlag, 1996.

[52] R. D. Hempstead and M. Lax, "Classical noise. VI. Noise in self-sustained oscillators near threshold," *Phys. Rev.*, vol. 161, pp. 350–366, Sep. 1967.

[53] D. Yuvaraj, M. B. Kadam, O. Shtempluck, and E. Buks, "Optomechanical cavity with a buckled mirror," *J. Microelectromech. Syst.*, vol. 22, no. 2, pp. 430–437, 2013.

[54] H. P. Hsu, *Schaum's Outline of Theory and Problems of Probability, Random Variables, and Random Processes*. New York, NY, USA: McGraw-Hill, 1997.

[55] D. W. Allan, "Statistics of atomic frequency standards," *Proc. IEEE*, vol. 54, no. 2, pp. 221–230, Feb. 1966.

[56] L. S. Cutler and C. L. Searle, "Some aspects of the theory and measurement of frequency fluctuations in frequency standards," *Proc. IEEE*, vol. 54, no. 2, pp. 136–154, Feb. 1966.
[57] F. Walls and D. Allan, "Measurements of frequency stability," *Proc. IEEE*, vol. 74, no. 1, pp. 162–168, Jan. 1986.

Ilya Baskin was born in 1980 in Ekibastuz, Kazakhstan (former Soviet Union). He received a B.Sc. in Electrical Engineering and a B.A. in Physics from the Technion–Israel Institute of Technology in Haifa, Israel, in 2003. He received the Ph. D degree from the same institution in 2011. His graduate research was focused on optical and microwave spectroscopy of quantum heterostructures.

In 2011, he joined the Quantum Electronics Laboratory, Technion, as a postdoctoral fellow where he is working on superconducting nanowire single photon detectors and micro opto-mechanic devices.

D. Yuvaraj received the Ph.D. degree from the Indian Institute of Science, Bangalore, India, in 2010.

From 2010 to 2012, he was a Postdoctoral Fellow with the Quantum Electronics Laboratory, Technion–Israel Institute of Technology, Haifa, Israel. He is currently in the pursuit of Majorana fermions in the semiconductor-superconductor interface at the London Centre for Nanotechnology, University College London, London, U.K. His research interests include integration of nanomaterials by nanofabrication for applications in nanoelectronics and integrated devices.

Gil Bachar was born in Tel-Aviv, Israel, in 1980. He received his B.A. degree in exact sciences in 2000 from the Open University in Israel. He received his M.Sc. degree in electrical engineering in 2009 from the Technion–Israel Institute of Technology in Haifa, Israel, where he is currently working toward the Ph.D. degree in electrical engineering. His research is focused on superconducting single photon detectors.

Keren Shlomi received the B.Sc. degree in electrical engineering in 2011 from the Technion–Israel Institute of Technology, Haifa, Israel, where she is currently working toward the M.Sc. degree in electrical engineering. Her research is focused on MOEMS devices.

Oleg Shtempluck was born in Moldova in 1949. He received the M.Sc. degree in electronic engineering from the Physical Department, Chernivtsi State University, Chernivtsi, Ukraine (former Soviet Union), in 1978.

He was a Team Leader with the Division of Design Engineering, Electronmash, from 1983 to 1992 and a Stamp and Mold Design Engineer with Ikar Company from 1992 to 1999, both in Ukraine. He is currently a Laboratory Engineer with the Microelectronics Research Center, Technion–Israel Institute of Technology, Haifa, Israel. His research concerns semiconductors and dielectrics.

Eyal Buks received the B.Sc. degree in mathematics and physics from Tel Aviv University, Tel Aviv, Israel, in 1991 and the M.Sc. and Ph.D. degrees in physics from the Weizmann Institute of Science, Rehovot, Israel, in 1994 and 1998, respectively. His graduate work concentrated on interference and dephasing in mesoscopic systems.

From 1998 to 2002, he was a Postdoctoral Scholar with the California Institute of Technology (Caltech), Pasadena, studying experimentally nanomachining devices. He is currently an Associate Professor with the Technion–Israel Institute of Technology, Haifa, Israel. His current research is focused on nanomachining and mesoscopic physics.